Met. Mater. Int., Vol. 21, No. 5 (2015), pp. 891~896
doi: 10.1007/s12540-015-5098-y

Effect of High-Pressure Torsion on the Microstructure and Wear Behavior of NiTi Alloy

Mohammad Farvizi[1,*], Mohammad Reza Akbarpour[2], Eun Yoo Yoon[3], and Hyoung Seop Kim[4]

[1]Ceramic Division, Materials and Energy Research Center, Tehran, P.O. Box 14155-4777, Iran
[2]Department of Materials Engineering, Faculty of Engineering, University of Maragheh, Maragheh, Iran
[3]Korea Institute of Materials Science (KIMS), Changwon 642-831, Korea
[4]Department of Materials Science and Engineering, Pohang University of Science and Technology, Pohang 790-784, Korea

(received date: 17 February 2015 / accepted date: 4 May 2015)

The wear property of NiTi is one of the most important properties of this alloy. In the current study, the effect of high-pressure torsion (HPT) process on the wear properties of an austenitic NiTi shape memory alloy is investigated. Full density NiTi samples with a composition of Ti-56 wt% Ni are fabricated using hot isostatic pressing (HIP), followed by the HPT process at room temperature, with an applied pressure of 6 GPa for 10 turns. The microstructural analysis reveals that the HIP-processed samples with a B2-NiTi phase evolve into significant grain refinement after HPT process and an interwoven B2-B19′ nanocrystalline/amorphous structure formed, leading to increased hardness in these samples. The results of the wear tests using a ball-on-disc configuration at room temperature demonstrate that the wear performance of the samples is improved after the HPT process. This is due to greater hardness and better pseudo-elasticity in the HPT-processed samples.

Keywords: shape memory alloys, severe plastic deformation, phase transformation, wear, scanning/transmission electron microscopy (STEM)

1. INTRODUCTION

Because of the interesting and unique properties they produce, severe plastic deformation (SPD) methods have recently been favored for manufacturing bulk nanomaterials. High-pressure torsion (HPT) is one of the most successful SPD methods. In this method, disc-shaped samples are subjected to high levels of applied pressure and torsion. This imposes extremely large strains on the target materials and yields ultrafine-grained structure, compared with other SPD methods [1].

Recently, various aspects of NiTi shape memory alloys, such as pseudo-elasticity (PE) and shape memory effect (SME), have been investigated [2]. Both PE and SME effects originate from a martensitic transformation between austenite (high-temperature) and martensite (low temperature) phases. The wear property of NiTi is one of the most important properties of this alloy [3]. Different hypotheses have been proposed to describe its extraordinary wear resistance. Some researchers [3,4] believe that the PE property is the main factor enhancing the wear resistance of the alloy under low loads. Some evidences show that this property cannot be very effective under high loads and long travel distances (during wear testing) where heavy plastic deformations induce in worn surfaces [5-7]. Under such a condition, other properties, for example hardness and strain hardening, play major roles in enhancement of wear resistance of the NiTi alloy.

There are numerous reports about the successful application of the HPT process for metals, intermetallics, and composites [8-10]. This method has also been employed for the production of bulk nanostructured NiTi. While different aspects of the HPT-processed NiTi, such as microstructure [11,12], mechanical properties [13], and corrosion behavior [14], have been well investigated, to the best of our knowledge, there is no report about the effect of employing the HPT process on the wear behavior of this alloy.

In this study, in order to understand the effects of the HPT process on the wear resistance of NiTi, first, full density NiTi samples with an austenitic structure at room temperature were consolidated using a hot isostatic pressing (HIP) method. Then they were subjected to the HPT process. The wear behavior of the samples before and after the HPT process was investigated.

2. EXPERIMENTAL PROCEDURES

High-purity pre-alloyed NiTi powders with a composition

*Corresponding author: mmfarvizi@yahoo.com, mmfarvizi@merc.ac.ir

of Ti-56wt%Ni and average particle size of 15 μm were used as raw materials. Stress-free transformation temperatures of the NiTi powders, which were measured using a differential scanning calorimetry (DSC) technique, are as follows: martensite start (M_s) temperature: 3 °C, martensite finish (M_f): -22 °C, austenite start (A_s): 6 °C, and austenite finish (A_f): 28 °C.

The HIP method was used to fabricate full density NiTi samples. The samples were consolidated at 1065 °C and 100 MPa for 3 h. The details of the HIP consolidation technique were presented elsewhere [15,16]. After preparing the full density NiTi samples via the HIP method, the samples were cut using electro discharge machining (EDM). Disc-shaped samples with a diameter of 10 mm and thickness of 0.8 mm were polished for the HPT process. The HPT process was performed according to Ref. [17]. The discs were placed between the HPT anvils and processed in the HPT facility at room temperature for 10 revolutions under an initial pressure of 6 GPa with a constant rotation speed of 1 rpm.

The microstructure of the samples, before and after the HPT process, was observed using optical microscopy (OM, Olympus). The phase characterization of the samples was conducted using an advanced Bruker X-ray diffractometer (XRD) with monochromatic Cu K_α radiation. Atomic resolution imaging of the samples were investigated using a CS-corrected STEM (JEM-2100F, JEOL, Japan) operated at 200 kV. The HRTEM specimens were prepared using dimpling and ion milling techniques.

The instrumented nanoindentation was carried out on an Agilent Technologies Nanoindenter 6200 using a three-sided Berkovich tip. At least ten indentations were conducted for each sample. Each indent was performed by loading to 30 mN over 20 s, holding at 30 mN for 10 s, fully unloading over 20 s, and holding at zero load for 60 s. Both the hardness and elastic modulus were determined from the recorded load-displacement curves using the software available with the Indentation Tester by the Oliver-Pharr method [18]. The pseudo-elasticity of the samples was measured according to the method described in Ref. [19].

The oscillating sliding wear tests were performed on a ball-on-flat tribometer at room temperature under unlubricated conditions. The system was equipped with sensors to automatically measure the wear depth. WC balls with a hardness of 75 HRC and a diameter of 5 mm were used as the counter friction pair. A 2 mm oscillating stroke and frequency of 5Hz, an applied load of 10 N and 300 m sliding distance were set for the wear test. Due to the thinness of the HPT-processed samples, higher applied loads during the wear tests were limited. All experiments were repeated three times to validate the results.

3. RESULTS AND DISCUSSION

Figure 1(a) represents the XRD pattern of the NiTi sample before the HPT process. It can be observed that the microstructure of the sample mainly consists of the B2-NiTi phase, which is in accordance with the initial composition of the starting powders. The XRD pattern of the NiTi sample after the HPT process in Fig. 1(b) demonstrates that after imposing heavy plastic deformation on the sample, two main changes occurred in the pattern. First, the width of the main peak (at 2θ=42.8°) was considerably broadened, which implies that a great grain refinement occurred and heavy strain was stored in the HPT-processed sample. Second, the intensity of the XRD peaks after the HPT process decreased, which indicates that the crystallinity of the sample decreased.

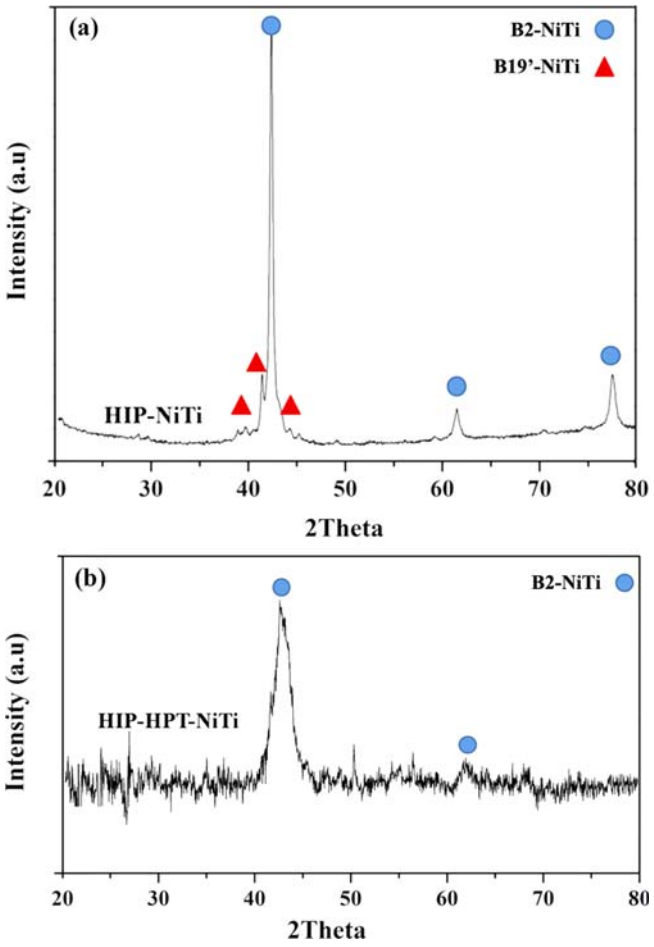

Fig. 1. XRD patterns of the NiTi samples (a) before and (b) after the HPT process.

Figure 2(a) shows an optical micrograph of the HIP-NiTi sample revealing the micro-size grains in the microstructure. After the HPT process, the grain size was reduced and reached the nanometric scale, as indicated in the Fig. 2(b).

To better evaluation of the microstructural changes that occurred during the HPT process, the microstructures of the samples before and after the HPT process were observed using the HRTEM technique. In Fig. 3, an HRTEM image

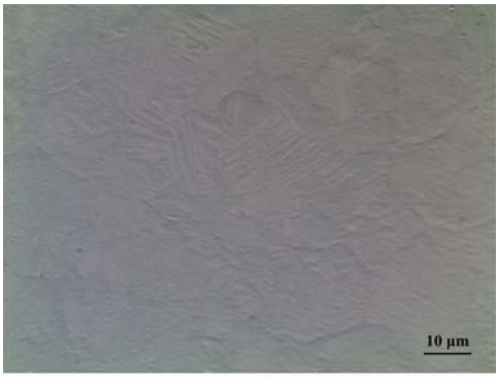

(a)

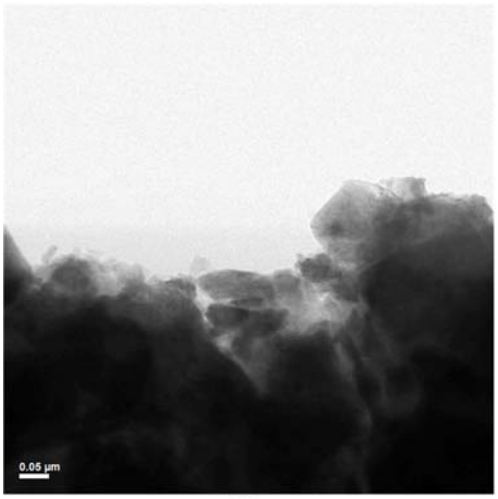

(b)

Fig. 2. (a) Optical micrograph of the HIP-NiTi sample and (b) HRTEM image of the HPT-HIP-NiTi sample.

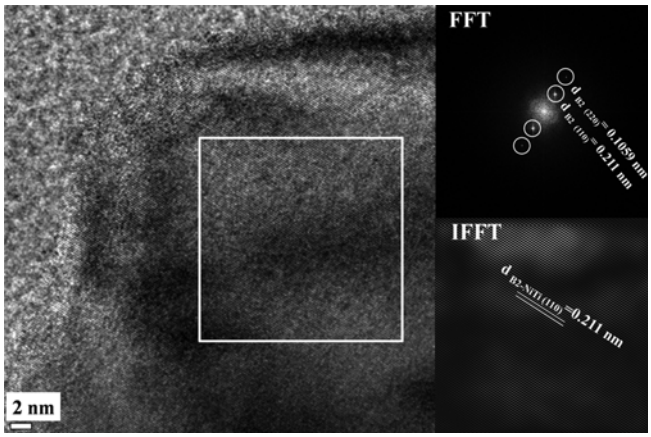

Fig. 3. HRTEM image of NiTi sample before HPT processing with corresponding FFT and IFFT micrographs.

of the NiTi sample before the HPT process is presented. The fast Fourier transform (FFT) image taken from the squared area and the corresponding inverse FFT micrograph confirm the existence of the austenitic B2 phase in this sample.

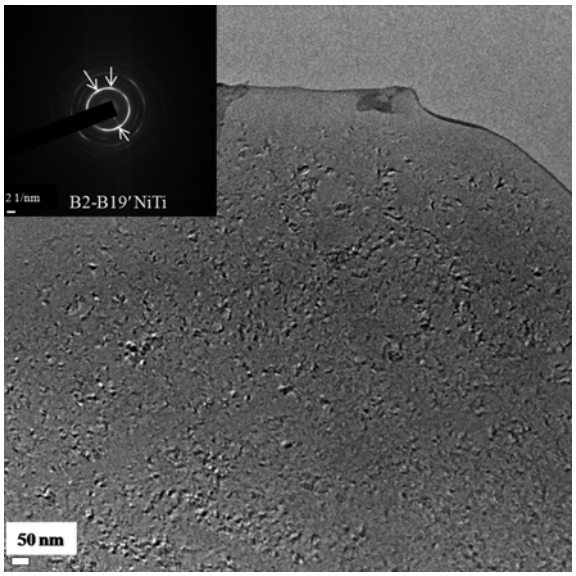

Fig. 4. HRTEM image of NiTi sample after HPT processing. The arrows mark spots of B19′ martensite phase.

In addition, the lattice defects (e.g., dislocations) were rarely observed.

However, after the HPT process, the microstructure of the NiTi samples was significantly altered. Figure 4 exhibits an HRTEM image of the HPT-processed NiTi sample. The corresponding diffraction pattern shows that both the B2 and B19′ NiTi phases coexist in the HPT-processed sample. It is well-known that imposing SPD methods will decrease the martensitic transformation temperatures and, as a consequence, enhances the austenite stability in NiTi [20,21]. It is believed that, formation of small fractions of the martensite phase in the HPT processed NiTi can be explained by the stress induced martensite (SIM) formation mechanism. During the HPT process, with the gradual increment of the stress SIM plates form and with further enhancement of the stress, these plates will stabilize in the microstructure. This feature was also observed in previous researches [22].

A higher magnification HRTEM image in Fig. 5 was used to characterize the HPT-processed sample in more detail. With the aid of the FFT and IFFT images, it was found that amorphization in some parts of the microstructure occurred due to dislocation accumulations during the HPT process [22]. Considering the HRTEM images, it can be concluded that an interwoven B2-B19′ NiTi/amorphous structure evolved during the HPT process. Moreover, it can be seen that the stress-induced martensite phase is at nano scale.

The nanoindentation test was employed in order to analyze the mechanical properties of the samples. The results of the tests for the NiTi samples before and after the HPT process are presented in Fig. 6 and Table 1. The test results demonstrate that the hardness increased after applying SPD via the HPT process. This was due to grain refinement in the HPT-

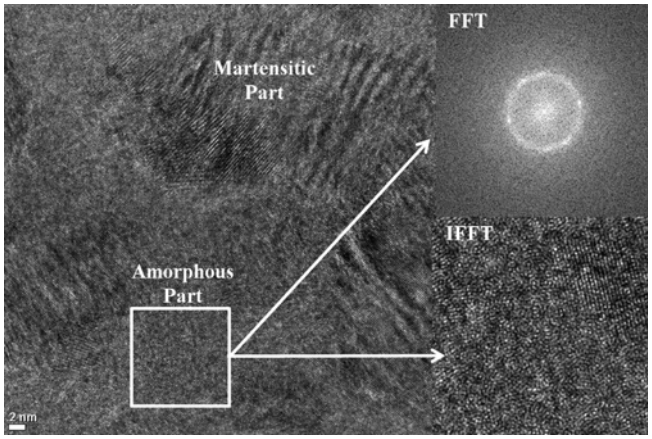

Fig. 5. Higher magnification HRTEM image from NiTi sample after HPT process.

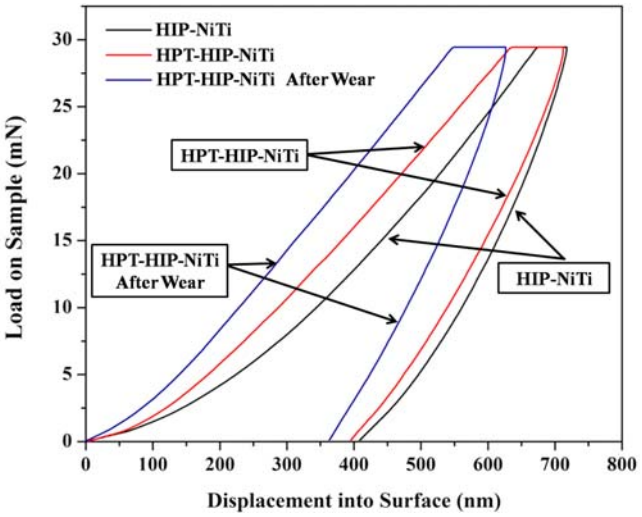

Fig. 6. Nanoindentation test results for NiTi samples before and after HPT process and after the wear test.

processed samples while pseudoelasticity did not decrease. Furthermore, indentation measurements across the HPT-processed sample area demonstrate that the hardness distribution was homogenous. The decrease in elastic modulus after the HPT process is due to phase amorphization and grain refinement to nanoscale [23].

In order to understand the effect of the HPT process on the wear resistance of the NiTi, wear tests were conducted. The variation of wear loss (depth of a wear track) with a sliding distance is depicted in Fig. 7(a). It is seen that, the

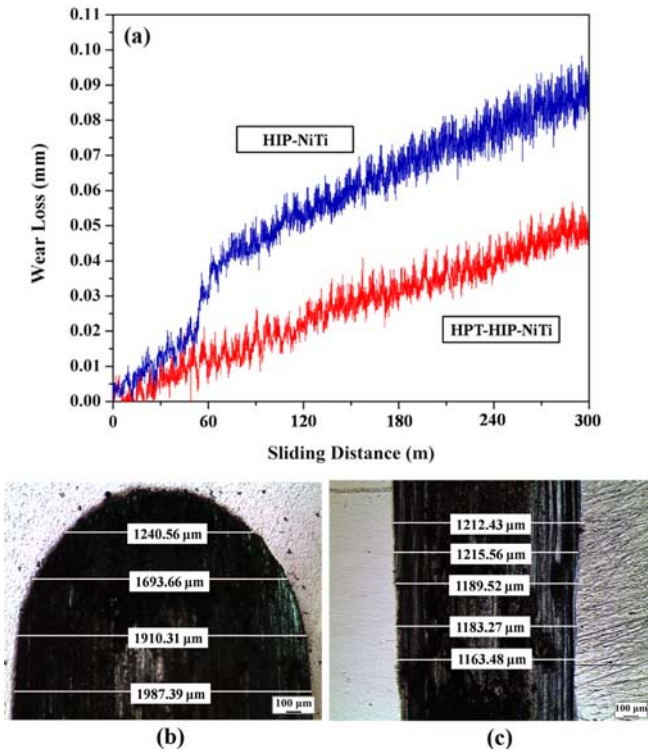

Fig. 7. (a) Variation of the wear loss (depth of wear track) with sliding distance under 10 N normal load, (b) Optical micrograph obtained from worn surface of NiTi sample before HPT, and (c) after HPT.

depth of the wear track considerably increased after 60 m sliding in the HIP-processed NiTi sample. This shows that the initial surface resistance to ploughing yields at this point and, consequently, the wear depth increases. With an increase in sliding distance after this point, the depth of the wear track increases steadily. However, after applying the HPT process to this sample, a significant improvement in the wear resistance was observed, and the HPT-processed sample had a shallower wear track for all sliding distances. In addition, measurements of the width of wear tracks confirmed the improved wear performance of the NiTi samples after the HPT process (Figs. 7b and 7c). Previous studies conducted on the wear resistance of NiTi showed that under higher loads, hardness plays a large role in the wear property of the NiTi alloy. This is due to heavy plastic deformation and temperature increment during wear tests [6,24]. In contrast, a combination of hardness and PE simultaneously control the wear resistance of this alloy under low loads. In this research, because

Table 1. Hardness, elastic modulus and pseudoelasticity values obtained from Fig. 6

	Nanohardness (GPa)	Microhardness (GPa)	Elastic Modulus (GPa)	Pseudoelasticity (η ratio) %
HIP-NiTi	3.60±0.3	3.85±0.2	52.06±8.5	46.9±1.1
HPT-HIP- NiTi	3.92±0.4	4.21±0.5	49.63±9.8	47.3±1.2
HPT-HIP- NiTi After wear test	4.92±0.6	4.98±0.5	60.62±9.2	42.3±1.4

of the thinness of the HPT-processed samples, wear tests were limited to lower normal loads (e.g., 10 N) for which both hardness and PE factors were important in the wear behavior of the alloy. According to the microhardness and nanoindentation results, despite the hardness increment after the HPT process, PE did not decrease. It is believed that the local relaxation of stress, caused by reversible martensitic transformation (pseudo-elasticity effect) during the wear test [5,24], can help to improve the wear resistance of the HPT-processed alloy. Moreover, the HPT-processed samples have a higher hardness than the HIP-processed NiTi samples. Being harder, and having a significant amount of PS effect, explains the superior wear performance of the HIP-HPT-processed samples. The results of the nanoindentation tests performed on the HPT-HIP-NiTi samples, after wear test, are shown in Fig. 6 and Table 1. It is seen that strain hardening occurs in the samples during wear process, which leads to the hardness increases. Also, the calculation of η ratio shows that the pseudoelasticity effect is slightly affected after the wear process, but the sample still has a much higher η ratio in comparison with normal materials (for example, in the case of 304 steel η ratio is %11 [25]) which confirms the occurrence of the medium stress relaxation and improvement of the wear resistance of the samples.

The results of the EDS analysis from the worn surfaces of the samples after 300 m sliding against WC balls indicated that no tungsten element was detected in the worn area of the NiTi before the HPT process, while 0.22 at% of W element was measured in the worn surface after applying the HPT process which may help the strain hardening process during wear tests. In another attempt for the production of nanostructured NiTi with the HPT method, cold-pressed NiTi samples subjected to HPT process. The cold-pressed HPTed samples failed to perform satisfactory during wear tests at similar conditions and heavy delamination observed in these samples which originates from weak welding between particles. This experiment approved the necessity of performing a pre-consolidation before HPT to attain a considerable wear performance.

4. CONCLUSIONS

In this study, in order to investigate the effect of the HPT process on the wear resistance of an austenitic NiTi alloy, first, full density NiTi samples were consolidated using the HIP method and then subjected to the HPT process. The following conclusions were deduced:

(1) The XRD results showed that after the HPT process, the width of peaks was broadened. This is attributed to grain refinement and strain increment in the HPT-processed samples.

(2) The microstructural studies performed using HRTEM showed that while the HIP-processed sample consists mainly of B2-NiTi phase, stress-induced martensite plates evolved after the HPT process in some areas. Moreover, amorphization due to dislocation accumulation has been observed in the HPT-processed microstructure.

(3) The nanoindentation and microhardness test results showed that after the HPT process, hardness increased by 8%, while pseudo-elasticity did not decrease.

(4) The wear tests proved the superior wear performance of the HPT-processed samples. This originated from the better mechanical properties of these samples.

ACKNOWLEDGEMENT

This work was supported by the National Research Foundation of Korea (NRF) grant funded by the Korea government (MSIP) (No. 2014R1A2A1A10051322).

REFERENCES

1. A. P. Zhilyaev and T. G. Langdon, *Prog. Mater. Sci*. **53**, 893 (2008).
2. K. Otsuka, X. Ren, *Prog. Mater. Sci.* **50**, 511 (2005).
3. D. Y. Li, *Wear* **221**, 116 (1998).
4. C. Zhang and Z. N. Farhat, *Wear* **267**, 394 (2009).
5. L. G. Korshunov, V. G. Pushin, N. L. Chernenko, and V. V. Makarov, *Phys. Met. Metallography* **110**, 91 (2010).
6. M. Farvizi, T. Ebadzadeh, M. R. Vaezi, H. S. Kim, and A. Simchi, *Mater. Design* **51C**, 375 (2013).
7. M. Farvizi, T. Ebadzadeh, M. R. Vaezi, E. Y. Yoon, Y.-J. Kim, J. Y. Kang, H. S. Kim, and A. Simchi, *Wear* **334-335**, 35 (2015).
8. E. Y. Yoon, D. J. Lee, B. H. Park, M. R. Akbarpour, M. Farvizi, and H. S. Kim, *Met. Mater. Int.* **19**, 927 (2013).
9. M. I. Abd El Aal, and H. S. Kim, *Mater. Design* **53**, 373 (2014).
10. Y. F. Sun, T. Nakamura, Y. Todaka, M. Umemoto, and N. Tsuji, *Intermetallics* **17**, 256 (2009).
11. R. Singh, S. V. Divinski, H. Rösner, E. A. Prokofiev, R. Z. Valiev, and G. Wilde, J. *Alloys Comp.* **509**, 290 (2011).
12. M. Peterlechner, T. Waitz, and H. P. Karnthaler, *Script. Mater.* **59**, 566 (2008).
13. H. Shahmir, M. Nili-Ahmadabadi, Y. Huang, and T. G. Langdon, *J. Mater. Sci.*, **49**, 2998 (2014).
14. F. L. Nie, Y. F. Zhenga, Y. Cheng, S. C. Wei, and R. Z. Valiev, *Mater. Letters* **64**, 983 (2010).
15. M. Farvizi, T. Ebadzadeh, M. R. Vaezi, E. Y. Yoon, Y.-J. Kim, H. S. Kim, and A. Simchi, *J. Alloy Comp.* **606**, 21 (2014).
16. L. Krone, E. Schüller, M. Bram, O. Hamed, H.-P. Buchkremer, and D. Stöver, *Mater. Sci Eng A* **378**, 185 (2004).
17. T. Waitz, V. Kazykhanov, and H. P. Karnthaler, *Mater. Sci. Eng. A* **52**, 137 (2004).
18. W. C. Oliver and G. M. Pharr, *J. Mater. Res*. **7**, 1564 (1992).
19. R. Liu and D. Y. Li, *Script. Mater.* **41**, 691 (1999).
20. Z. Fan and C. Xie, *Mater. Letters* **62**, 800 (2008).

21. Z. Li, G. Xiang and X. Cheng, *Mater. Design* **27**, 324 (2006).
22. S. D. Prokoshkin, I. Y. Khmelevskaya, S. V. Dobatkin, I. B. Trubitsyna, E. V. Tatyanin, V. V. Stolyarov, and E. A. Prokofiev, *Acta Mater.* **53**, 2703 (2005).
23. S. R. Agnew and J. R. Weertman, *Mater. Sci. Eng. A* **242**, 174 (1998).
24. D. Y. Li, *Wear* **255**, 617 (2003).
25. H. Z. Ye, R. Liu, and R. Eadie, *Scrip. Mater.* **41**, 1039 (1999).